type 3 complexes of Ni^{2+} (1.84 Å)[8] and Cu^{2+} (1.86–1.87 Å).[9] The longer bond lengths from Co^{2+} to ethereal oxygen atoms, indicating, as expected, a weaker interaction, are consistent with those found previously (2.17, 2.33 Å) in an octahedral Co^{2+} complex of a neutral, macrocyclic ligand.[15]

(ii) Bond lengths to the two imino nitrogen atoms are 2.13–2.14 Å, significantly shorter than those to ethereal oxygen atoms but slightly longer than metal–nitrogen distances that we have found in four-coordinate complexes of Ni^{2+} (1.90 Å)[8] or Cu^{2+} (2.00–2.03 Å).[9]

(iii) The two nitrogen atoms are in essentially linear coordination to Co^{2+} (178–179°) with the two alkoxy oxygen atoms in positions very close to the plane perpendicular to the N–Co–N axis; O–Co–N angles are in the range 88–92°. However, the O–Co–O angle *within* this plane is no less than 121.6°, a gross departure from octahedral geometry. In fact, this side of the molecule is better described in terms of trigonal-bipyramidal geometry around Co^{2+}, with the nitrogen atoms occupying axial sites and the alkoxy oxygen atoms on two equatorial sites.

(iv) The two ethereal oxygen atoms, O(2) and O(3), are approximately 0.6 Å above and below the plane defined by the alkoxy oxygens and Co^{2+}. The O–Co–O bite angle in the central five-membered ring is unusually low at 69–70°; more usual values in systems of this type are 75.5° on Co^{2+},[15] 78.7° on Ni^{2+},[16] and 73° on Mn^{2+}.[17]

It appears that the steric requirements of the multiply chelated ligand, in conjunction with the weak interactions between the metal ion and the ethereal oxygen atoms, have distorted the geometry around Co^{2+} to the point where it is intermediate between octahedral six-coordination and a five-coordinate structure where O(2) and O(3) share one corner of a trigonal-bipyramidal arrangement. The relationship of this structure to the postulated trans-bridged square-planar geometry of **17** may easily be seen; it is only necessary to increase the O(1)–Co–O(4) angle to approximate linearity, while removing O(2) and O(3) to nonbonding distances, in order to produce a four-coordinate structure.

(15) Armstrong, L. G.; Lindoy, L. F.; McPartlin, M.; Mockler, G. M.; Tasker, P. A. *Inorg. Chem.* **1977**, *16*, 1665.
(16) Drummond, L. A.; Henrick, K.; Kanagasundaram, M. J. L.; Lindoy, L. F.; McPartlin, M.; Tasker, P. A. *Inorg. Chem.* **1982**, *21*, 3923.
(17) Drew, M. G. B.; Othman, A. H. B.; McFall, S. G.; McIlroy, P. D. A.; Nelson, S. M. *J. Chem. Soc., Dalton Trans.* **1977**, 1173.

Conclusions

This work has shown that the template condensation of the fluorinated keto alcohol $HOC(CF_3)_2CH_2C(O)CH_3$ with the amino group is of general applicability in the preparation of metal complexes of potentially polydentate, iminoalkoxy, Schiff-base type ligands. However, the actual mode of coordination of the ligand and geometry of the resulting metal complex are influenced by small differences in the donor strength of the potentially coordinating atoms, the chain length and geometry of the ligand molecule, and the steric preferences of the metal ion. In the case of Co^{2+}, where the steric requirements of the d^7 metal ion are not strongly defined, the geometry of a six-coordinate complex is dominated by the need to accommodate a set of five linked chelate rings. In other instances, some potential donor sites remain uncoordinated in the ultimate complex, but there is evidence that their presence has influenced the course of the condensation reaction.

Acknowledgment. Financial support of this work was provided by the Natural Sciences and Engineering Research Council of Canada.

Registry No. **5**, 88412-35-5; **6**, 88412-36-6; **7**, 88412-37-7; **8**, 88412-39-9; **9**, 88425-08-5; **10**, 88412-40-2; **11**, 88412-41-3; **12**, 88412-43-5; **14**, 88412-42-4; **15**, 88412-44-6; **16**, 929-59-9; **17**, 88412-45-7; **18**, 88425-09-6; **19**, 88412-46-8; **20**, 88412-47-9; **21**, 88412-48-0; **22**, 88412-49-1; **23**, 88412-50-4; **24**, 88412-51-5; $NH_2(CH_2)_3NH(CH_2)_2NH(CH_2)_3NH_2 \cdot 4HCl$, 13493-17-9; $NH_2(CH_2)_2O(CH_2)_2NH_2$, 2752-17-2; HFDA, 10487-10-2; 1,2-bis(2-hydroxyethoxy)ethane, 112-27-6.

Supplementary Material Available: Tables of temperature factors, hydrogen atom coordinates, bond angles and distances associated with the CF_3 groups, and values of $10|F_o|$ and $10|F_c|$ (35 pages). Ordering information is given on any masthead page.

Contribution from the Department of Chemistry, University of Colorado, Boulder, Colorado 80309

Steric Effects in Electron-Transfer Reactions. 1. Trends in Homogeneous Rate Constants for Reactions between Members of Structurally Related Redox Series

CARL A. KOVAL,* ROBIN L. A. PRAVATA, and CINDY M. REIDSEMA

Received June 24, 1983

Three series of structurally related inorganic complexes based on $Ru(NH_3)_5(py)^{3+,2+}$, $Co(1,10\text{-phen})_3^{3+,2+}$, and $Cu(H_{-2}\text{-triglycine})^{0,-}$ have been prepared. The remaining members of each series contain organic substituents, methyl, cyclohexyl, bis(hydroxymethyl)methyl, or tris(hydroxymethyl)methyl, in place of hydrogens located on the periphery of the ligands. Each complex displays a one-electron redox couple that involves the III and II oxidation states of the metal. Formal reduction potentials are reported in 0.2 M NaCl. Electron-transfer reaction rate constants for all possible cross-reactions between the Ru(III) and Co(II) complexes and between the Cu(III) and Co(II) complexes are reported. The dependence of the magnitude of these rate constants on the free energy change for the reaction and on the size of the reactants is analyzed by using the concepts of Marcus' theory. For the Ru(III) + Co(II) reactions, large organic substituents result in a reduction in the rate constants with respect to values calculated with use of Marcus' theory, whereas for the Cu(III) + Co(II) reactions the steric effects are less predictable.

Introduction

During the last three to four decades, numerous theoretical and experimental studies have been directed toward understanding the factors that influence the rates of electron-transfer reactions in solution.[1-3] Reactions involving transition-metal complexes have played a key role in many of these studies because the orbital from which an electron originates and the orbital to which it is transferred are identified with single atoms. Furthermore, the wide variety of available ligands

(1) Sutin, N. *Acc. Chem. Res.* **1982**, *15*, 275; **1968**, *8*, 225.
(2) Marcus, R. A. *Annu. Rev. Phys. Chem.* **1964**, *15*, 155.
(3) Creutz, C.; Endicott, J. F.; Haim, A.; Meyer, T. J.; Sutin, N. *Prog. Inorg. Chem.* **1983**, *30*, 1, 141, 273, 389, 441.

0020-1669/84/1323-0545$01.50/0

allows subtle control over such factors as exothermicity and reorganization energies. To a large extent, the ligands also determine the distance over which the electron transfer occurs. This latter consideration has become increasingly important as attempts are made to unravel the complexities of electron-transfer reactions in biological systems and in photoinduced electron-transfer reactions that occur in natural and synthetic solar energy conversion systems.[4]

In contrast to what is known about how ligands influence the energetic factors associated with electron transfer, relatively little is known about ligand-induced steric factors, especially for bimolecular reactions. Investigations of electron transfer within mixed-valence, binuclear complexes have provided a detailed picture of intramolecular electron transfer,[5] but the precursor complexes for many intermolecular reactions can never achieve a structurally stable bridge between the donor and acceptor metal centers. Nevertheless, steric interactions between two reacting complexes may be a factor in the reaction rate and may be a dominant factor when large ligands are involved.

One way that large ligands could influence electron-transfer rates between metal ions is by preventing sufficient overlap between the donor and acceptor orbitals. Should this occur, the rate would be less than that predicted on the basis of energetic factors. Within the framework of the accepted models describing electron transfer, such sterically inhibited reactions are called nonadiabatic.[1-3] Taube has reviewed the evidence for nonadiabatic electron-transfer reactions involving complex ions and has concluded that, except for a few examples, steric effects are not required to explain the observed rates.[6] It can be argued, however, that relatively few attempts have been made to vary ligand structure systematically so that steric effects can be identified.

We are investigating the importance of steric effects in homogeneous and heterogeneous electron-transfer reactions by synthesizing series of structurally related complexes that vary only in the size of organic substituents that are bonded to the ligands in positions remote from the donor atoms. Within each series, energetic factors associated with metal-based redox couples should remain constant or vary in a predictable way so that steric effects, which may be relatively small, can be discovered and studied. In this paper we report the kinetics of homogeneous electron-transfer reactions involving complexes that are derivatives of pentaammine(pyridine)ruthenium, tris(phenanthroline)cobalt, and (triglycine)copper. Each of these parent complexes displays a M(III, II) redox couple and each has been shown to undergo outer-sphere electron-transfer reactions.[7-18] The organic substituents used to induce steric effects are relatively small: methyl, cyclohexyl, bis(hydroxymethyl)methyl, and tris(hydroxymethyl)methyl. Furthermore, in two of the three series the substituents are not spherically distributed. Trends in the observed rate constants suggest that the larger organic substituents inhibit the rate of electron transfer.

Experimental Section

Reagents and Materials. Triglycineamide (G_3a) and trialanine (A_3) were purchased from Vega Biochemicals. A sample of tri-α-aminoisobutyric acid (Aib_3) was donated by A. W. Hamburg and D. W. Margerum, Chemistry Department, Purdue University, West Lafayette, IN. The compounds 1-amino-1-cyclohexanecarboxylic acid (Ach), (((*tert*-butoxycarbonyl)oxy)imino)phenylacetonitrile (BOC-ON), diethyl cyanophosphonate (DEPC), and 1,10-phenanthroline monohydrate (phen) were purchased from Aldrich. These chemicals were used without further purification. 4,7-Dimethyl-1,10-phenanthroline (4,7-Me_2phen) was obtained from G. Frederick Smith Chemical Co. and recrystallized from water. Other chemicals and solvents were reagent grade. Argon was passed through consecutive towers containing V(II)/Zn(0) in HCl and distilled water.

Synthesis of Organic Ligands. The ligand 4-(tris(hydroxymethyl)methyl)pyridine (4-thmpy) was synthesized from 4-methylpyridine (4-Mepy) according to the procedure of Koenigs and Happe.[19] The crude product was recrystallized from tetrahydrofuran or dioxane; yield based on 4-methylpyridine 90%. ^{1}H NMR (Me_2SO-d_6): δ 8.52 (d, 2 H), 7.50 (d, 2 H), 4.55 (t, 3 H, –OH), 3.74 (d, 6 H, $-CCH_2O-$).

4,7-Bis(bis(hydroxymethyl)methyl)-1,10-phenanthroline (4,7-(bhm)$_2$phen). 4,7-Dimethyl-1,10-phenanthroline (7.6 g, 34 mmol) was placed in a constricted tube (i.d. = 20 mm, o.d. = 24 mm). After aqueous formaldehyde (37%) (27 g, 0.34 mol) was added, the tube was sealed and placed in a boiling water bath for 72 h. The tube was placed in ice and opened without difficulty because very little pressure had built up during the reaction. Steam was passed through the reaction mixture until an equal volume of water was collected. Solvent was removed from the remaining liquid by evaporation, and the residue was dissolved in boiling methanol or ethanol. The alcohol was evaporated to remove any remaining formaldehyde, and the remaining residue was dissolved in twice its volume of boiling methanol. After cooling, the precipitate was removed by filtration and recrystallized in the minimum amount of methanol. The crystals were washed with anhydrous ether, dried in vacuo, and stored at room temperature; yield based on 4,7-Me_2phen 67%, ^{1}H NMR (Me_2SO-d_6): δ 9.03 (d, 2 H), 8.30 (s, 2 H), 7.70 (d, 2 H), 4.80 (b s, 4 H, –OH); 3.88 (b s, 10 H, –CH and $-CCH_2$). ^{13}C NMR (Me_2SO-d_6): δ 148.9, 147.9, 146.0, 127.2, 121.7, 121.2, 62.2, 44.7.

$NH_2C(C_5H_{10})(CO)OCH_2C_6H_5 \cdot CH_3C_6H_4SO_3H$ (AchOBz·TOSH). Benzene (25 mL), benzyl alcohol (100 mL), *p*-toluenesulfonic acid (0.121 mol), and 1-amino-1-cyclohexanecarboxylic acid (0.121 mol) were combined in a flask fitted with a Dean–Stark trap. The mixture was allowed to reflux until no more water accumulated in the trap (8–10 h). The contents of the flask were allowed to cool and were then poured into diethyl ether (250 mL). The white crystals that formed were recrystallized from a mixture of ethyl acetate and methanol; yield based on 1-amino-1-cyclohexanecarboxylic acid 70%. ^{1}H NMR (Me_2SO-d_6): δ 7.56 (d, 2 H, phenyl), 7.46 (s, 5 H, phenyl), 7.16 (d, 2 H, phenyl), 5.30 (s, 2 H, $-CH_2-$), 2.30 (s, 3 H, $-CH_3$), 1.66 (b, 10 H, cyclohexyl).

$(CH_3)_3CO(CO)NHC(C_5H_{10})COOH$ (BOCAch). 1-Amino-1-cyclohexanecarboxylic acid (0.250 mol) was added to a solution of NaOH (0.375 mol) in water (150 mL). After dissolution, acetone (150 mL) was added, followed by BOC-ON (0.250 mol). The mixture was stirred for 3 h at room temperature followed by 3 h of stirring in a water bath at 40–50 °C. Water (150 mL) was added to the reaction mixture, and the acetone was evaporated. The aqueous solution was extracted with ethyl acetate (3 × 100 mL). The ethyl acetate remaining in the aqueous fraction was removed by evaporation, and the aqueous fraction was chilled and acidified with solid citric acid. The off-white, sticky solid that formed was recrystallized from a mixture of ethyl acetate and pentane, resulting in white, needlelike crystals; yield based on 1-amino-1-cyclohexanecarboxylic acid 68%. ^{1}H NMR (Me_2SO-d_6): δ 6.85 (b, 1 H, –NH), 1.66 (b, 10 H, cyclohexyl), 1.36 (s, 9 H, $-C(CH_3)_3$).

(4) Chance, B., Devault, D. C., Frauenfelder, H., Marcus, R. A., Schrieffer, J. B., Sutin, N., Eds. "Tunneling in Biological Systems"; Academic Press: New York, 1979.
(5) Meyer, T. J. *Acc. Chem. Res.* **1978**, *11*, 94.
(6) Taube, H. "Bioinorganic Chemistry-II"; Raymond, K., Ed.; American Chemical Society: Washington, D.C., 1977; Adv. Chem. Ser. No. 162, p 127–144.
(7) Brown, G. M.; Sutin, N. *J. Am. Chem. Soc.* **1979**, *101*, 883.
(8) Chou, M.; Creutz, C.; Sutin, N. *J. Am. Chem. Soc.* **1977**, *99*, 5615.
(9) Brown, G. M.; Krentzien, H. J.; Abe, M.; Taube, H. *Inorg. Chem.* **1979**, *18*, 3374.
(10) Farina, R.; Wilkins, R. G. *Inorg. Chem.* **1967**, *7*, 514.
(11) Baker, B. R.; Basolo, F.; Neumann, H. M. *J. Phys. Chem.* **1959**, *63*, 371.
(12) Owens, G. D.; Chellappa, K. L.; Margerum, D. W. *Inorg. Chem.* **1979**, *18*, 960.
(13) Dekorte, J. M.; Owens, G. D.; Margerum, D. W. *Inorg. Chem.* **1979**, *18*, 1538.
(14) Lappin, A. G.; Youngblood, M. P.; Margerum, D. W. *Inorg. Chem.* **1980**, *19*, 407.
(15) Owens, G. D.; Margerum, D. W. *Inorg. Chem.* **1981**, *20*, 1446.
(16) Koval, C. A.; Margerum, D. W. *Inorg. Chem.* **1981**, *20*, 2311.
(17) Anast, J. M.; Margerum, D. W. *Inorg. Chem.* **1982**, *21*, 3494.
(18) Anast, J. M.; Hamburg, A. W.; Margerum, D. W., to be submitted for publication.
(19) Koenigs, W.; Happe, G. *Chem. Ber.* **1903**, *36*, 2904.

$(CH_3)_3CO(CO)[NHC(C_5H_{10})(CO)]_2OCH_2C_6H_5$ (BOCAch$_2$OBz). AchOBz·TOSH (28.6 mmol) was dissolved in 1 M K_2CO_3 (200 mL) and was extracted with ethyl acetate (3 × 75 mL). The ethyl acetate solution was dried over $MgSO_4$, filtered, and evaporated. Dimethylformamide (90 mL) was added to the residual oil, followed by BOCAch (31.5 mmol). This mixture was chilled in an ice bath, and diethyl cyanophosphonate (31.5 mmol) in dimethylformamide (10 mL) was added dropwise with stirring, followed by dropwise addition of triethylamine (62.9 mmol) in dimethylformamide (10 mL). After 3 h of stirring in the ice bath, the mixture was allowed to come to room temperature and was then stirred for an additional 18 h. Benzene (220 mL) and ethyl acetate (880 mL) were added to the reaction mixture. This solution was extracted with 10% citric acid (3 × 110 mL), water (1 × 110 mL), saturated NaCl (1 × 110 mL), saturated $NaHCO_3$ (2 × 110 mL), water (2 × 110 mL), and saturated NaCl (2 × 110 mL). The organic fraction was dried over $MgSO_4$, filtered, and evaporated, resulting in a yellow oil. This oil was crystallized from ethyl acetate/hexane and recrystallized from ethanol/water; yield based on AchOBz·TOSH 50%. ^1H NMR ($CDCl_3$): δ 7.36 (s, 5 H, phenyl), 7.36 (b, 1 H, -NH), 5.12 (s, 2 H, $-CH_2-$), 4.56 (b, 1 H, -NH), 1.66 (b, 20 H, cyclohexyl), 1.42 (s, 9 H, $-C(CH_3)_3$).

$(CH_3)_3CO(CO)[NHC(C_5H_{10})(CO)]_3OCH_2C_6H_5$ (BOCAch$_3$OBz). BOCAch$_2$OBz (4.4 mmol) was stirred in trifluoroacetic acid (10 mL) for 1 h. The excess trifluoroacetic acid was evaporated, and ethyl acetate (20 mL) was added to the oily residue. The solution was slowly made basic with 1 M Na_2CO_3. The fractions were separated, and the aqueous phase was extracted with ethyl acetate (2 × 10 mL). All of the ethyl acetate fractions were combined, dried over $MgSO_4$, filtered, and evaporated. The resulting oil was dissolved in dimethylformamide (14 mL), and BOCAch (4.8 mmol) was added to this solution. This mixture was chilled in an ice bath, and diethyl cyanophosphonate (4.8 mmol) in dimethylformamide (2 mL) was added dropwise with stirring, followed by dropwise addition of triethylamine (9.6 mmol) in dimethylformamide (2 mL). After 3 h in the ice bath, the mixture was allowed to come to room temperature and was then stirred for an additional 18 h. Benzene (36 mL) and ethyl acetate (144 mL) were added to the reaction mixture, and this solution was extracted with 10% citric acid (3 × 50 mL), water (1 × 18 mL), saturated NaCl (1 × 18 mL), saturated $NaHCO_3$ (2 × 18 mL), water (2 × 18 mL), and saturated NaCl (2 × 18 mL). The organic fraction was dried over $MgSO_4$, filtered, and evaporated, resulting in a yellow oil. The product was purified by flash chromatography using a solvent mixture of ethyl acetate and hexane;[20] yield based on BOCAch$_2$OBz 50%. ^1H NMR ($CDCl_3$): δ 7.68 (b, 1 H, -NH), 7.30 (s, 5 H, phenyl), 6.46 (b, 1 H, -NH), 5.06 (s, 2 H, $-CH_2-$), 4.82 (b, 1 H, -NH), 1.66 (b, 30 H, cyclohexyl), 1.40 (s, 9 H, $-C(CH_3)_3$).

$(CH_3)_3CO(CO)[NHC(C_5H_{10})(CO)]_3OH$ (BOCAch$_3$). PdO catalyst[21] (37.6 mg) was suspended in methanol (10 mL), and H_2 gas was passed through the suspension until the catalyst formed clumps. BOCAch$_3$OBz (0.75 mmol) and glacial acetic acid (4 drops) were added to the suspension, and hydrogen bubbling was continued until thin-layer chromatography (ethyl acetate/hexane) indicated the disappearance of BOCAch$_3$OBz. Methanol (80 mL) was added with slight heating to dissolve the precipitated product, the PdO catalyst was removed by filtration, and the solution was evaporated to dryness. (*Caution*! Addition of solvent to the dried catalyst can cause fires.) The resulting solid was washed with ethyl acetate; yield based on BOCAch$_3$OBz 91%. ^1H NMR (Me_2SO-d_6): δ 7.25 (b, 1 H, -NH), 6.95 (b, 1 H, -NH), 6.82 (b, 1 H, -NH), 1.66 (b, 30 H, cyclohexyl), 1.42 (s, 9 H, $-C(CH_3)_3$).

H[NHC(C_5H_{10})(CO)]$_3$OH·CF_3COOH (Ach$_3$·TFA). Solid BOCAch$_3$ (0.68 mmol) was stirred in trifluoroacetic acid (TFA) (5 mL) for 1 h. The excess TFA was evaporated, and the solid residue was recrystallized from ethyl acetate/hexane; yield based on BOCAch$_3$ 74%. ^1H NMR (Me_2SO-d_6): δ 7.76 (b, 1 H, -NH), 7.02 (b, 1 H, -NH), 1.66 (b, 30 H, cyclohexyl).

All synthesized ligands gave satisfactory microanalyses.

Preparation of Inorganic Complexes. $[Ru(NH_3)_5Cl]Cl_2$ was prepared as described by Vogt,[22] and $Ru(NH_3)_5(H_2O)(PF_6)_2$ was prepared as described by Callahan.[23] $Ru(NH_3)_5(py)(ClO_4)_2$ and

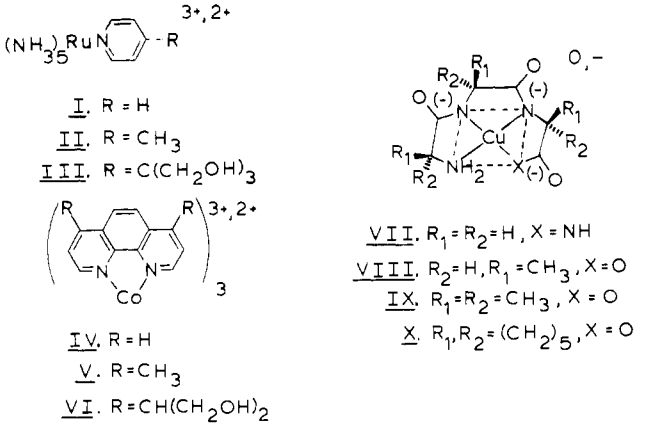

Figure 1. Structural drawings and symbols for the complexes that compose the three redox series.

$Ru(NH_3)_5(4\text{-Mepy})(ClO_4)_2$ were prepared by the procedure of Ford.[24] The synthesis of $Ru(NH_3)_5(thmpy)(PF_6)_2$ was accomplished by using the following procedure. In a typical preparation, $Ru(NH_3)_5(H_2O)(PF_6)_2$ (0.123 g, 0.250 mmol) was placed in a 50-mL round-bottom flask that had been fitted with a serum cap. The flask was deaerated with argon for 15 min. A second 50-mL round-bottom flask containing 4-thmpy (0.10 g, 0.55 mmol) was also fitted with a serum cap and deaerated with argon for 10–15 min. Deaerated acetone (10 mL) was added to the $Ru(NH_3)_5(H_2O)(PF_6)_2$ while deaerated methanol (5 mL) was added to the 4-thmpy. The acetone solution was slowly added to the stirred methanol solution by using a cannula. This combined solution was protected from light and stirred for 10–15 min. Cold anhydrous ether (40 mL) was added until cloudiness signaled the beginning of precipitate formation. The solution was then chilled at 4 °C for approximately 2 h. The precipitate, removed by filtration, was washed twice with cold anhydrous ether and dried in a vacuum desiccator.

The Ru(II) complexes were characterized by their electronic spectra and electrochemistry. Each complex displayed a single charge-transfer band near 400 nm. The band maxima and molar absorptivities were in close agreement with previously reported values. Each complex displayed a single oxidation wave between −0.4 and +1.0 V vs. SSCE.

Tris(1,10-phenanthroline)cobalt(II), tris(4,7-dimethyl-1,10-phenanthroline)cobalt(II), and tris(4,7-bis(bis(hydroxymethyl)-methyl)-1,10-phenanthroline)cobalt(II) were prepared in solution. A $Co(ClO_4)_2$ stock solution was prepared from $CoCO_3$ and $HClO_4$ and was standardized gravimetrically by precipitation of Co(II) with $Hg(SCN)_4^{2-}$. The ligand was dissolved in an aqueous solution that contained the amounts of NaCl and NaOAc necessary to achieve final concentrations of 0.2 and 0.005 M, respectively. These solutions were adjusted to pH 5.0 with HCl and deaerated with argon. The appropriate volume of the $Co(ClO_4)_2$ stock solution was added to the ligand solution so that the molar ratio of ligand to cobalt was 3.2/1. At the concentration levels used, $1-5 \times 10^{-4}$ M in Co^{2+}, the excess ligand ensures complete formation of the tris complexes. The solutions were deaerated for an additional 10 min prior to use.

Solutions of $Cu^{II}(H_{-3}G_3a)^-$, $Cu^{II}(H_{-2}A_3)^-$, $Cu^{II}(H_{-2}Aib_3)^-$, and $Cu^{II}(H_{-2}Ach_3)^-$ were prepared by combining the appropriate volume of a $Cu(ClO_4)_2$ stock solution with a 25% excess of the tripeptide and enough NaCl to result in a 0.2 M solution. The pH was then adjusted to 8.5–10.5 with NaOH. The $Cu(ClO_4)_2$ stock solution was prepared from $CuCO_3$ and $HClO_4$ and standardized by titration with EDTA to a murexide endpoint. The Cu(III) tripeptide solutions were prepared by electrochemical oxidation of the Cu(II) tripeptide solutions using a flow system employing a powdered graphite working electrode packed in a porous glass tube, wrapped externally with a platinum-wire counterelectrode.[25] After electrolysis, the solutions were diluted with a 0.005 M acetate buffer at pH 5 that was 0.2 M in NaCl. For reactions involving oxygen-sensitive cobalt solutions, the buffer was

(20) Still, W. C.; Kahn, M.; Mitra, A. *J. Org. Chem.* **1978**, *43*, 1978.
(21) Shriner, R. L.; Adams, R. J. *J. Am. Chem. Soc.* **1924**, *46*, 1683.
(22) Vogt, L. H.; Katz, J. L.; Wiberley, S. E. *Inorg. Chem.* **1965**, *4*, 1157.
(23) Callahan, R. W.; Brown, G. M.; Meyer, T. J. *Inorg. Chem.* **1975**, *14*, 1443.
(24) Ford, P.; Rudd, D. P.; Gaunder, R.; Taube, H. *J. Am. Chem. Soc.* **1968**, *90*, 1187.
(25) Clark, B. R.; Evans, D. H. *J. Electroanal. Chem.* **1965**, *69*, 181.

deaerated with argon prior to the dilution. Solutions of Cu(III) tripeptide complexes are photosensitive requiring the use of darkroom lights during kinetic experiments.[26]

Homogeneous Kinetic Measurements. Rate constants for the electron-transfer reactions between the metal complexes were measured by using a Durrum stopped-flow spectrophotometer interfaced to a Digital Equipment Corp. MINC-11 computer. The rates of reactions between the Cu(III) complexes and the Co(II) complexes were measured by monitoring the loss of absorbance due to the Cu(III) species (approximately 395 nm). The rates of reactions involving ruthenium and cobalt complexes were monitored at λ_{max} for the Ru(II) species (approximately 400 nm). For reactions involving $Co(phen)_3^{3+,2+}$ the disappearance of Ru(II) was observed while for reactions involving $Co(4,7\text{-}Me_2phen)_3$ and $Co(4,7\text{-}(bhm)_2phen)^{3+,2+}$ the appearance of Ru(II) was observed. In all reactions, the concentration of the cobalt complex was at least 10 times greater than the copper or ruthenium complex concentration resulting in pseudo-first-order kinetics. First-order kinetic traces were observed for all reactions for at least 3 reaction half-lives indicating that reaction orders for the copper or ruthenium complexes were unity. Reaction orders for the cobalt complexes were determined from order plots that invariably indicated reaction orders of 1 for the excess reagent.

During each kinetic run, 250 absorbance measurements were digitized at constant time intervals with the total time corresponding to at least 3 reaction half-lives. Typically, absorbance vs. time data for three kinetic runs were collected, and the ensemble was then averaged. The data for each set of runs was subjected to linear and nonlinear analysis[27] that yielded a pseudo-first-order rate constant, k_{obsd}, the initial absorbance, A_0, and the final absorbance, A_{inf}, described by the equations

$$\ln (A - A_{inf}) = -k_{obsd}t + \ln (A_0 - A_{inf})$$

$$-d[M(III)]/dt = k_{obsd}[M(III)]$$

Three values of k_{obsd}, which typically differed by less than 10%, were averaged for each set of experimental conditions.

For reactions involving the Cu(III) complexes where k_{obsd} exceeded 200 s^{-1}, rate constants were simply estimated from the absorbance vs. time data itself. The uncertainty in these values is probably ±50%.

Electrochemical Measurements. Formal reduction potentials for the various redox couples were measured with use of cyclic voltammetry at platinum or glassy-carbon working electrodes utilizing a PAR 371 potentiostat/galvanostat, a PAR 379 digital coulometer, a PAR 175 universal programmer, and a Houston Omnigraphic X-Y recorder. At the slow sweep rates used (50–200 mV/s), all couples yielded nearly reversible waves and E_f was taken to be the average of the anodic and cathodic peak potentials. For the ruthenium and cobalt complexes, the values of E_f determined by cyclic voltammetry were checked by using potentiometry. Constant-potential electrolysis at a platinum-gauze electrode was used to prepare solutions with various M(III)/M(II) concentration ratios. The potentials of these solutions were recorded, and values of E_f vs. SSCE were evaluated from the Nernst equation. The agreement between the values of E_f determined by cyclic voltammetry and potentiometry was within a few millivolts.

Instrumentation. Electronic spectra were recorded on a Cary 219 spectrophotometer. Elemental Analyses were performed by Atlantic Microlabs, Inc., Atlanta, GA.

Results

Electronic Spectra and Formal Reduction Potentials. Table I summarizes the visible spectra for the M(II) oxidation states of the complexes in water and lists the formal reduction potentials for the M(III)/M(II) couples in 0.2 M aqueous NaCl. Values of λ_{max} for the intense LMCT bands in the Cu(III) complexes are included. These data indicate that substitution of methyl, tris(hydroxymethyl)methyl, bis(hydroxymethyl)-methyl, or cyclohexyl groups for hydrogen on the ligands has small or predictable effects on these properties. The visible spectra of the members of the Ru(II) and Co(II) series are nearly identical. Although these data are not included in Table I, spectra of the Co(III) complexes are similar to each other and featureless from 300 to 800 nm. As with other Cu(III) tripeptide complexes, $Cu^{III}(H_{-2}Ach_3)$ exhibits two intense (ϵ = 5000–7000 M^{-1} cm^{-1}) charge-transfer bands. The position of λ_{max} for the Cu(II) complexes will be discussed later.

Table I. Electronic Spectra and Formal Reduction Potentials

complex	λ_{max}, nm	E_f vs. SSCE,[b] V
$Ru(NH_3)_5(py)^{2+}$	406	0.053[c] (0.069)[38]
$Ru(NH_3)_5(4\text{-Mepy})^{2+}$	398	0.016[c]
$Ru(NH_3)_5(4\text{-thmpy})^{2+}$	409	0.045[c]
$Co(phen)_3^{2+}$	430–450 sh[a]	0.114[c] (0.144)[39]
$Co(4\text{-}Me_2phen)_3^{2+}$	430–450 sh[a]	−0.089[c]
$Co(4\text{-}(bhm)_2phen)_3^{2+}$	430–450 sh[a]	−0.024[c]
$Cu(H_{-2}G_3a)^0$	365	0.404[d] (0.404)[28]
$Cu(H_{-2}G_3a)^-$	555	
$Cu(H_{-2}A_3)^0$	270, 385	0.574[d] (0.574)[28]
$Cu(H_{-2}A_3)^-$	543	
$Cu(H_{-2}Aib_3)^0$	278, 395	0.424[d] (0.424)[28]
$Cu(H_{-2}Aib_3)^-$	508	
$Cu(H_{-2}Ach_3)^0$	302, 396	0.284[d]
$Cu(H_{-2}Ach_3)^-$	498	

[a] Shoulders for $Co(4,7\text{-}(bhm)_2phen)_3^{2+}$ and $Co(4,7\text{-}Me_2phen)_3^{2+}$ are more pronounced than for $Co(phen)_3^{2+}$. [b] For the reduction of M(III) to M(II). [c] In 0.2 M NaCl buffered at pH 5.0 with 5 mM NaOAc. [d] In 0.2 M NaCl at pH 9.0.

Formal reduction potentials for the redox couples involved in the cross reactions were measured by cyclic voltammetry and potentiometry allowing accurate equilibrium constants for these reactions to be calculated. Where comparisons are possible, these values of E_f agree well with values from the literature.

The reduction potential for $Cu^{III,II}(H_{-2}Ach_3)^{0,-}$ is the most negative value reported for a Cu tripeptide complex. Bossu and Margerum were able to correlate reduction potentials for similar complexes with λ_{max} for the Cu(II) form of the complex.[28] If their correlation is used to predict E_f for $Cu^{II}(H_{-2}Ach_3)^{0,-}$ from λ_{max}, a value of 0.272 V vs. SSCE is obtained. This prediction agrees well with the measured value, 0.284 V. Bossu also developed a list of additive contributions for various α substituents, which allows values of E_f to be estimated. Our data indicate that the contribution for each Ach residue is 0.140 V, which is significantly greater than the contribution of two α-alkyl substituents, 0.080 V. It is possible that steric interactions between the cyclohexyl group and peptide backbone force the deprotonated peptide nitrogens to be stronger σ donors, which will tend to stabilize Cu(III) with respect to Cu(II).[28]

Complex Formation, Solubility, and Stability. In general, the presence of substituents on the ligands did not have an obvious effect on the rate of formation of the metal complexes. Formation of the Ru(II) complexes began immediately upon addition of the pyridine ligands to solutions of $Ru(NH_3)_5(H_2O)^{2+}$ and the reactions were complete within $^1/_2$ h. Similarly, addition of $Co(H_2O)_6^{2+}$ to a solution of the phenanthroline ligands produced a bright yellow solution within a few seconds.

The formation of Cu(II) tripeptide complexes usually occurs rapidly when base is added to solutions of $Cu(H_2O)_6^{2+}$ and the tripeptide ligands. The complexes are relatively stable under mildly basic conditions (pH 8.5–10.5). While $Cu(H_{-2}Ach_3)^-$ forms rapidly in basic solutions, the complex itself is not stable for long periods of time as evidenced by the

(26) While solutions of Cu(III) complexes are photosensitive, decomposition within the observation chamber of the stopped-flow spectrophotometer was not significant on the time scale of the electron-transfer reactions. For a complete description of the photodecomposition of Cu(III) peptide complexes, see: Hamburg, A. W.; Margerum, D. W., to be submitted for publication in *Inorg. Chem.*

(27) The analysis program was adapted from the program used by Margerum and co-workers in ref 12–18.

(28) Bossu, F. P.; Chellappa, K. L.; Margerum, D. W. *J. Am. Chem. Soc.* **1977**, *99*, 2195.

Table II. Homogeneous Electron-Transfer Rate Constants

oxidant	reductant	K_{12}[a]	k_{12}[b]
$Ru(NH_3)_5(py)^{3+}$	$Co(phen)_3^{2+}$	9.3×10^{-2}	1.6×10^{2} [c]
	$Co(4,7\text{-}Me_2phen)_3^{2+}$	260	3.2×10^{3}
	$Co(4,7\text{-}(bhm)_2phen)_3^{2+}$	20	2.1×10^{3}
$Ru(NH_3)_5(4\text{-}Mepy)^{3+}$	$Co(phen)_3^{2+}$	2.2×10^{-2}	9.7×10^{1} [c]
	$Co(4,7\text{-}Me_2phen)_3^{2+}$	61	2.8×10^{3}
	$Co(4,7\text{-}(bhm)_2phen)_3^{2+}$	4.8	9.0×10^{2}
$Ru(NH_3)_5(4\text{-}thmpy)^{3+}$	$Co(phen)_3^{2+}$	6.8×10^{-2}	1.2×10^{2} [c]
	$Co(4,7\text{-}Me_2phen)_3^{2+}$	190	2.3×10^{3}
	$Co(4,7\text{-}(bhm)_2phen)_3^{2+}$	15	7.8×10^{2}
$Cu(H_{-2}G_3a)$	$Co(phen)_3^{3+}$	7.9×10^{4}	2.2×10^{5}
	$Co(4,7\text{-}Me_2phen)_3^{2+}$	2.1×10^{8}	6×10^{6}
	$Co(4,7\text{-}(bhm)_2phen)_3^{2+}$	1.7×10^{7}	1.2×10^{6}
$Cu(H_{-2}A_3)$	$Co(phen)_3^{2+}$	6.0×10^{7}	1.9×10^{6}
	$Co(4,7\text{-}Me_2phen)_3^{2+}$	1.6×10^{11}	1×10^{7} [d]
	$Co(4,7\text{-}(bhm)_2phen)_3^{2+}$	1.3×10^{10}	5×10^{6} [d]
$Cu(H_{-2}Aib_3)$	$Co(phen)_3^{2+}$	1.8×10^{5}	4.9×10^{4}
	$Co(4,7\text{-}Me_2phen)_3^{2+}$	4.7×10^{8}	1.1×10^{6}
	$Co(4,7\text{-}(bhm)_2phen)_3^{2+}$	3.8×10^{7}	7.6×10^{5}
$Cu(H_{-2}Ach_3)$	$Co(phen)_3^{2+}$	1.0×10^{3}	6.0×10^{4}
	$Co(4,7\text{-}Me_2phen)_3^{2+}$	2.8×10^{6}	3.0×10^{6}
	$Co(4,7\text{-}(bhm)_2phen)_3^{2+}$	2.2×10^{5}	1.5×10^{5}

[a] Calculated from values of E_f in Table I. [b] M^{-1} s^{-1}. [c] $k_{12} = K_{12}k_{21}$. [d] Estimated from absorbance vs. time trace.

precipitation of $Cu(OH)_2$. The decomposition apparently involves the hydrolysis of the peptide ligand because the $Cu^{II}(H_{-2}Ach_3)^-$ complex can not be re-formed by acidifying the solution followed by the addition of base.

The Co(II) complexes derived from phen and 4,7-Me_2phen were found to be relatively insoluble ($<10^{-4}$ M) in solutions that were 0.2 M in $LiSO_3CF_3$, $NaClO_4$, or KPF_6. This insolubility dictated the use of NaCl in this study. Anions such as ClO_4^- are preferable for kinetic studies involving charged species because these anions are less likely to cause ion-pairing effects. In this respect, the solubility of complexes derived from ligands containing hydroxymethyl groups warrants further mention. Solutions can readily be prepared that contain 1 mM $Ru^{II}(NH_3)_5(thmpy)^{2+}$ or $Co^{II}(4,7\text{-}(bhm)_2phen)_3^{2+}$ in 0.5 M $NaClO_4$.

All of the Co(II) and Ru(II) complexes can be oxidized to the M(III) state and later reduced back to the M(II) state by using controlled-potential electrolysis (CPE). In all cases, the total charge required to oxidize the complex was nearly equal to the charge required in the subsequent reduction ($Q_f = Q_r$). Use of Faraday's law revealed that n was equal to 1 for each electrode process. Electronic spectra recorded before and after the CPE experiments indicate a small amount of decomposition for the Ru(III) complexes.[29]

Like $Cu^{III}(H_{-2}Aib_3)$, $Cu^{III}(H_{-2}Ach_3)$ is very stable in solution in the absence of light and moderately stable (hours) in ambient light. When these Cu(III) solutions are irradiated with a 150-W mercury lamp, the bright yellow color due to Cu(III) disappears within a few minutes.

Homogeneous Electron-Transfer Reactions. Cross-reaction rate constants, k_{12}, for all possible reactions between the cobalt complexes and the ruthenium and copper complexes were measured by using stopped-flow spectrophotometry. In all cases the reaction stoichiometry was assumed to be

$$\text{Ru(III) (or Cu(III))} + \text{Co(II)} \underset{k_{21}}{\overset{k_{12}}{\rightleftharpoons}} \text{Ru(II) (or Cu(II))} + \text{Co(III)}$$

All reactions were found to be first order with respect to the M(II) and M(III) reactants. For the reactions between the ruthenium complexes and $Co^{II}(phen)_3^{3+,2+}$, the equilibrium constant for the reaction written above is less than 1. In these cases, the rate constant k_{21} was measured and k_{12} is reported as $K_{12}k_{21}$. Values of k_{12} and K_{12} are listed in Table II.

Table III. Effect of Ionic Strength on Cross-Reaction Rate Constants

[NaCl], M	μ	$10^{-5} \times k_{12}$[a] for IX + VI	[NaCl], M	μ	$10^{-5} \times k_{12}$[a] for IX + VI
0.001	0.006	6.4	0.501	0.506	8.7
0.051	0.056	6.8	1.001	1.006	10
0.201	0.206	7.6			
[NaCl], M	μ	$10^{-3} \times k_{12}$[a] for I + IV	[NaCl], M	μ	$10^{-3} \times k_{12}$[a] for I + IV
0.004	0.009	0.23	0.504	0.509	4.3
0.054	0.059	0.80	1.004	1.009	6.7
0.204	0.209	2.1			

[a] M^{-1} s^{-1}.

The data in Table II are in good agreement with previously reported kinetic data,[8,13] except for the reaction of $Ru(NH_3)_5(py)^{3+}$ + $Co(4,7\text{-}Me_2phen)_3^{2+}$. McArdle et al. studied the reaction in the reverse direction and reported $k_{21} = 3.0 \times 10^2$ M^{-1} s^{-1},[30] whereas our data can be used to calculate $k_{21} = 12$ M^{-1} s^{-1}. It is not clear whether McArdle was aware that $Ru^{III}(NH_3)_5(py)^{3+}$ is a stronger oxidant than $Co^{III}(4,7\text{-}Me_2phen)_3^{3+}$. Plots of k_{obsd} vs. [excess reagent] with nonzero intercepts were reported and were attributed to photochemical decomposition of $Ru^{II}(NH_3)_5(py)^{2+}$, but which may have been due to reversible kinetics. The authors of this previous study noted problems associated with precipitation of $Co^{III}(4,7\text{-}Me_2phen)_3Cl_3$. The Co(II) form of this complex is soluble below 0.2 mM in 0.2 M NaCl, but we found solutions of this complex to be air sensitive. Reproducible kinetic results using this complex could be obtained only if solutions of the ligand were deaerated with argon prior to the addition of $Co^{II}(H_2O)_6^{2+}$ and if all solutions were deaerated prior to the stopped-flow experiments.

Ionic Strength Effects. Rate constants for the reactions of $Cu^{III}(H_{-2}Aib_3)$ and $Ru(NH_3)_5(py)^{3+}$ with $Co(4,7\text{-}(bhm)_2phen)_3^{2+}$ were measured as a function of ionic strength. These data are presented in Table III. As expected, the reaction involving the uncharged Cu(III) complex is virtually unaffected by changes in chloride ion concentration and ionic strength. The slight trend that is observed could be due to changes in the formal reduction potentials for the two complexes. These results also indicate that chloride ion was not providing a mediating bridge in the reactions involving the square-planar copper complexes.

For the Ru(III)–Co(II) cross-reactions, a plot of log k_{12} vs. $\mu^{1/2}/(1 + \mu^{1/2})$ shows significant curvature; however, a tangent drawn through the data at the lowest ionic strength had approximately the slope predicted for a reaction involving 3+ and 2+ ions. The ionic strength dependence of this reaction is similar to what has been found in other studies where Debye–Hückel theory has been used for the calculation of work terms.[7]

Discussion

Calculation of Cross-Reaction Rate Constants Using Marcus' Theory. In order to examine possible steric effects for the observed cross-reaction rate constants, k_{12}^{obsd}, values of k_{12} that are corrected for work terms and the effect of driving force were calculated by using Marcus' theory.[2,31] Equations 1–9

(29) We observed that solutions of the Ru(III) complexes were much more stable in an electrochemical cell with the electrode potential poised several tenths of 1 V positive of E_f than in a normal container.

(30) McArdle, J. V.; Yocum, K.; Gray, H. B. *J. Am. Chem. Soc.* **1977**, *99*, 4141.

$$k_{12} = Z_{12} \exp(-\Delta G^*_{12}/RT) \quad (1)$$

$$\Delta G^*_{12} = \Delta G^{**}_{12} + w_{12} \quad (2)$$

$$Z_{12} = N[8\pi k_b T(m_1 + m_2)/m_1 m_2]^{1/2} \bar{r}_{12}^2/1000 \quad (3)$$

$$w = z_1 z_2 e^2/D_s \bar{r}(1 + \beta\mu^{1/2}\bar{r}) \quad (4)$$

$$\Delta G^{**}_{12} = (\Delta G^{**}_{11} + \Delta G^{**}_{22})/2 + \Delta G_r^\circ(1 + \alpha)/2 \quad (5)$$

$$\Delta G^{**}_{11} = \Delta G^*_{11} - w_{11} \quad (6)$$

$$\Delta G^{**}_{22} = \Delta G^*_{22} - w_{22} \quad (7)$$

$$\Delta G_r^\circ = \Delta G_{12}^\circ - w_{12} + w_{21} \quad (8)$$

$$\alpha = \Delta G_r^\circ/4(\Delta G^{**}_{11} + \Delta G^{**}_{22}) \quad (9)$$

were used in the calculation of k_{12}^{calcd}. In the equations above, N is Avogadro's number, k_b is the Boltzmann constant, β is the Debye–Hückel constant (0.329 in water at 298 K), μ is the ionic strength, R is the ideal gas constant, T is the absolute temperature, e is the electronic charge, and D_s is the static dielectric constant of the solvent. The subscript 12 refers to cross-reactions in the forward direction, the subscript 21 refers to the reverse of the cross-reaction, and the subscripts 11 and 22 refer to the appropriate self-exchange reactions. The quantity Z in eq 3 is a collision frequency where m and z refer to the masses and charges of the reactants, respectively. The free energy terms with the double asterisk denote the components of the activation free energies that do not include the work required to form precursor or successor complexes. Similarly, ΔG_{12}° and ΔG_r° represent the reaction free energy change before and after correction for work terms. These work terms were calculated from eq 4. Equations that are analogous to eq 1–4 can be written for the self-exchange reactions if appropriate subscripts are used.

The quantity $\bar{r}_{12}$ is the average reaction distance, which in all cases is assumed to be equal to the sum of the average radii of the reactants. The average radii, $\bar{r}$, for the cobalt and ruthenium complexes were assumed to be independent of the oxidation state of the metal and calculated by using the equation $\bar{r} = {}^1/_2(d_x d_y d_z)^{1/3}$ where the d's represent diameters along perpendicular axes.[41] These values were estimated from CPK molecular models. Since the Cu(II) forms of the peptide complexes probably have axially coordinated water molecules in aqueous solution,[40] the above formula is reasonable for calculating $\bar{r}$. The Cu(III) forms do not appear to have axial ligands,[40] and the molecular shape resembles a triangular prism instead of an ellipsoid. For this reason, the formula $\bar{r} = (3bhw/8\pi)^{1/3}$, where b and h represent the base and altitude of the triangular prism and w represents the thickness of the prism, was used to estimate the radii of the Cu(III) complexes.[41] Estimates of $\bar{r}$ for the various complexes are included in Table IV, and these values are in reasonable agreement with those used previously.[7,17,32]

Inspection of eq 1–9 reveals that cross-reaction rate constants, k_{12}, can be calculated by using values of ΔG^{**}_{11} and ΔG^{**}_{22} for the appropriate self-exchange reactions. Calculating values of ΔG^{**}_{11} for the self-exchange reactions involving couples where the self-exchange rate constant has been measured is straightforward using equations analogous to eq 1–4. Values of k_{11} are available for $Ru(NH_3)_5(py)^{3+,2+}$, $Co(phen)_3^{3+,2+}$, and $Cu(H_{-2}Aib_3)^{0,-}$.[9,33,16] When they are corrected to an ionic strength of 0.2 M and 298 K with use of the Debye–Hückel–Brønsted relationship, these values are 1.8×10^5, 24, and 5.5×10^5 M^{-1} s^{-1}, respectively.

Two values of ΔG^{**}_{11} for each remaining couple were estimated by using two different assumptions.

Assumption A is that the organic substituents have no effect on k_{11} and that the experimentally determined values given above can be used for an entire series. From this assumption, slight differences in ΔG^*_{11} and ΔG^{**}_{11} for the members of a series resulted from differences in work terms and collision frequencies. These quantities are listed in Table IV.

Assumption B is that the organic substituents produce differences in ΔG^{**}_{11} for the members of a series as well as differences in the work terms and collision frequencies. The quantity ΔG^{**} is often divided into an inner-sphere and outer-sphere component according to eq 10–12, where f_1 and

$$\Delta G^{**} = \Delta G^*_{in} + \Delta G^*_{out} \quad (10)$$

$$\Delta G^*_{in} = 6 f_1 f_2 (\Delta a^\circ)^2/2(f_1 + f_2) \quad (11)$$

$$\Delta G^*_{out} = (e^2/4)(1/2\bar{r}_{11} + 1/2\bar{r}_{22} - 1/\bar{r}_{12})(1/n^2 - 1/D_s) \quad (12)$$

f_2 are the breathing force constants of the two reactants, Δa° is the difference between the equilibrium metal–ligand bond distances of the two reactants, $\bar{r}_{11}$ and $\bar{r}_{22}$ are the radii of the reacting species, and n is the refractive index of the solvent. Assumption B is that the quantity $\Delta G^*_{11,in}$ for a series of complexes is constant but that $\Delta G^*_{11,out}$ changes according to the size of the complex as shown in eq 12. Assumption B, therefore, involves the calculation of a single value of $\Delta G^*_{11,in}$ for each series of couples and uses eq 12 to calculate $\Delta G^*_{11,out}$ for each couple. Equations 10, 2, and 4 can then be used to calculate ΔG^{**}_{11} and ΔG^*_{11}. For the cobalt and ruthenium series, the values of $\Delta G^*_{11,in}$ were calculated by using the known self-exchange rate constants for $Co(phen)_3^{3+,2+}$ and $Ru(NH_3)_5(py)^{3+,2+}$ together with eq 1–4, 12, and 10. The values so derived are 10.2 and 0.8 kcal/mol, respectively.

Since additional data are available, a more elaborate procedure was used to calculate $\Delta G^{**}_{11,in}$ for the copper complexes. Koval and Margerum reported rate constants for a series of pseudo-self-exchange reactions involving complexes derived from three tripeptides, two tripeptide amides, and a tetrapeptide ester.[17] For each reaction, values of $\bar{r}$ and Z were calculated as described above. With w_{12} equal to zero for reactions involving an uncharged species and on the assumption that $\Delta G^*_{11,in} = \Delta G^*_{22,in}$, eq 5 can be expanded by using eq 10 to yield

$$\Delta G^*_{12} = (\Delta G^*_{11,out} + \Delta G^*_{22,out})/2 + \Delta G^*_{in} + \Delta G_{12}^\circ(1 + \alpha)^2 \quad (13)$$

From eq 13, 1, 3, and 12, values of $\Delta G^{**}_{11,in}$ can be calculated for the nine pseudo-self-exchange reactions and one self-exchange reaction.[34] The average value of $\Delta G^*_{11,in}$ is 4.2 ± 0.4 kcal/mol.

Values of $\Delta G^*_{11,out}$, ΔG^{**}_{11}, and ΔG^*_{11} calculated by using assumption B are included in Table IV. The various parameters in Table IV can be used in conjunction with eq 1–9 to calculate cross-reaction rate constants for the reactions reported herein. The results of these calculations, $k_{12}^{calcd,A}$ from assumption A and $k_{12}^{calcd,B}$ from assumption B, are included in Table V.

Trends in the Rate Constants. According to Marcus' theory, the major factor affecting the rates of the cross-reactions will be the reaction free energy, ΔG_{12}°. This effect is usually represented in a plot of $\log k_{12}^{obsd}/f^{1/2}$ vs. $\log K_{12}$, which should be linear with a slope of 0.5 and an intercept of 0.5 $\log k_{11}k_{22}$ according to the Marcus correlation equations

$$k_{12} = (k_{11}k_{22}K_{12}f)^{1/2} \quad (14)$$

$$\log f = (\log K_{12})^2/[4 \log (k_{11}k_{22}/Z_{12}^2)] \quad (15)$$

(31) Marcus, R. A. *J. Chem. Phys.* **1965**, *43*, 679.
(32) Cummins, D.; Gray, H. B. *J. Am. Chem. Soc.* **1977**, *99*, 5158.
(33) Brücker, S.; Crescenzi, V.; Quadrifoglio, F. *J. Chem. Soc. A* **1970**, 1168.

(34) A constant value of $\Delta G^{**}_{11} = \Delta G^{**}_{22}$ obtained by using assumption A was used to calculate α.

Table IV. Calculated Parameters for Self-Exchange Reactions

couple	$\bar{r}$,[a] Å	$10^{-11}Z_{11}$[c]	w_{11}[d,g]	assumption A[e] ΔG^*_{11}[g]	assumption A[e] ΔG^{**}_{11}[g]	assumption B[f] ΔG^{**}_{out}[g]	assumption B[f] ΔG^{**}_{11}[g]	assumption B[f] ΔG^*_{11}[g]
I	3.8	2.4	1.6	8.4	6.8	6.0	6.8	8.4
II	3.9	2.4	1.5	8.4	6.9	5.8	6.6	8.1
III	4.1	2.4	1.4	8.4	7.0	5.6	6.4	7.8
IV	6.9	5.2	0.6	14.1	13.5	3.3	13.5	14.1
V	7.7	6.1	0.5	14.2	13.7	3.0	13.2	13.7
VI	9.1	6.9	0.4	14.3	13.9	2.5	12.7	13.1
VII	3.7, 4.3[b]	2.7	0	9.1	9.1	5.7	9.9	9.9
VIII	4.4, 4.6[b]	3.2	0	9.2	9.2	5.1	9.3	9.3
IX	4.7, 4.8[b]	3.3	0	9.2	9.2	4.8	9.0	9.0
X	5.2, 5.4[b]	3.5	0	9.3	9.3	4.3	8.5	8.5

[a] Calculated as described in text. [b] Cu(III), Cu(II). [c] M^{-1} s^{-1}, calculated with eq 3. [d] Calculated with eq 4. [e] Assuming k_{11} for each redox series is constant. [f] Assuming $\Delta G^{**}_{11,in}$ for each redox series and using eq 12 to calculate $\Delta G^{**}_{11,out}$. [g] kcal mol^{-1}.

Table V. Calculated Cross-Reaction Rate Constants[a]

reaction	ΔG_{12}°	w_{12}	w_{21}	$\bar{r}_{12}$	$10^{-11}Z_{12}$	$k_{12}^{calcd,A}$	$k_{12}^{calcd,B}$
I + IV	1.4	0.9	0.9	10.7	4.0	9.4×10^2	9.1×10^2
I + V	−3.3	0.8	0.8	11.5	4.5	5.1×10^4	7.8×10^4
I + VI	−1.8	0.7	0.7	12.9	5.4	2.0×10^4	5.3×10^4
II + IV	2.3	0.9	0.9	10.8	4.0	4.3×10^2	5.0×10^4
II + V	−2.4	0.8	0.8	11.6	4.5	2.5×10^4	4.7×10^4
II + VI	−0.9	0.7	0.7	13.0	5.4	9.5×10^3	3.1×10^4
III + IV	1.6	0.9	0.9	11.0	3.8	7.1×10^2	1.1×10^3
III + V	−3.1	0.8	0.8	11.8	4.3	3.8×10^4	9.7×10^4
III + VI	−1.6	0.7	0.7	13.2	5.0	1.4×10^4	6.3×10^4
VII + IV	−6.7	0	−0.4	10.6	4.0	5.1×10^5	2.7×10^5
VII + V	−11.4	0	−0.4	11.4	4.6	7.1×10^6	9.3×10^6
VII + VI	−9.9	0	−0.3	12.8	5.5	4.1×10^6	5.8×10^6
VIII + IV	−10.6	0	−0.4	11.3	4.3	7.1×10^6	6.9×10^6
VIII + V	−15.3	0	−0.4	12.1	4.9	1.1×10^8	1.6×10^8
VIII + VI	−13.8	0	−0.3	13.5	5.7	4.5×10^7	1.1×10^8
IX + IV	−7.2	0	−0.4	11.6	4.4	6.9×10^6	8.4×10^5
IX + V	−11.8	0	−0.4	12.4	4.9	1.4×10^7	2.6×10^7
IX + VI	−10.3	0	−0.3	13.8	5.7	5.3×10^6	1.6×10^7
X + IV	−4.1	0	−0.4	12.1	4.3	7.0×10^4	1.3×10^5
X + V	−8.8	0	−0.3	12.9	4.8	1.8×10^6	5.3×10^6
X + VI	−7.3	0	−0.3	14.3	5.5	6.0×10^5	3.0×10^6

[a] Free energies and work terms in kcal mol^{-1}; rate constants in M^{-1} s^{-1}; Z in M^{-1} s^{-1}; $\bar{r}_{12}$ in Å.

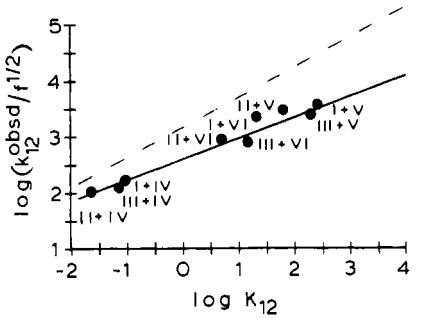

Figure 2. Marcus plot for the Ru(III) + Co(II) reactions using the data in Table II.

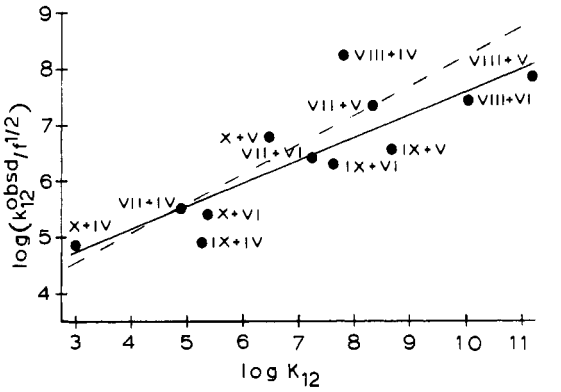

Figure 3. Marcus plot for the Cu(III) + Co(II) reactions using the data in Table II.

The data for the Ru(III) + Co(II) and Cu(III) + Co(II) reactions are plotted in this fashion in Figures 2 and 3. In each case the actual slope (solid line) is roughly equal to 0.4. Electron-transfer reactions involving Co(III, II) often yield slopes that are less than the value predicted by Marcus' theory.[8,10,13,30,35]

The deviation of the slope from 0.5 leads to intercept values that do not agree well with the values that can be calculated from known self-exchange rate constants for $Ru(NH_3)_5(py)^{3+,2+}$, $Co(phen)_3^{3+,2+}$, and $Cu(H_{-2}Aib_3)^{0,-}$. The dashed lines in Figures 2 and 3 have a slope of 0.5 and go through the calculated intercepts. We conclude that the dependence of the rate constants on driving force for these reactions is typical for reactions involving cobalt phenanthroline complexes.

Inspection of Figures 2 and 3 reveals a tendency for reactions involving sterically hindered complexes to deviate farthest from the theoretical lines. These steric effects are more evident in Figures 4 and 5 where the ratios of the calculated cross-reaction rate constants to the observed values are plotted against the estimated reaction distances, $\bar{r}_{12}$. In Figure 4, which contains data for the Ru(III) + Co(II) reactions, the ratios using both assumption A and B are displayed, whereas in Figure 5, which contains the data for the Cu(III) + Co(II)

(35) Rillema, D. P.; Endicott, J. F. J. Am. Chem. Soc. 1972, 94, 8711.

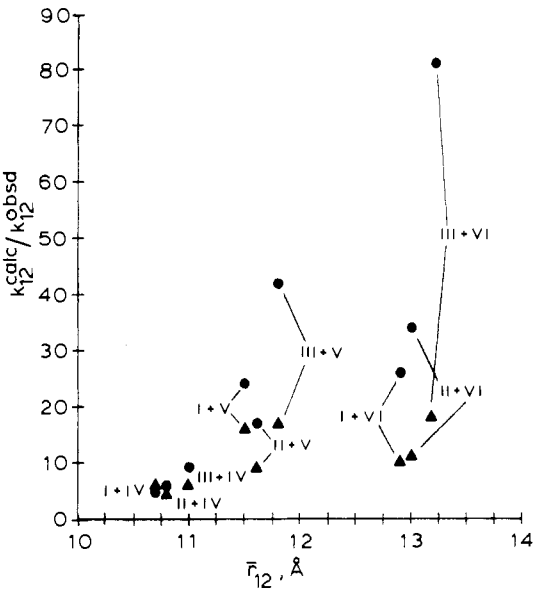

Figure 4. Plot of $k_{12}^{calcd}/k_{12}^{obsd}$ vs. $\bar{r}_{12}$ for the Ru(III) + Co(II) reactions. $\bar{r}_{12} = \bar{r}_{11} + \bar{r}_{22}$ (Table IV). Roman numerals indicate the reactants from Figure 1. Triangles are for k_{12}^{calcd} according to assumption A and circles are for k_{12}^{calcd} according to assumption B (see Table V and text).

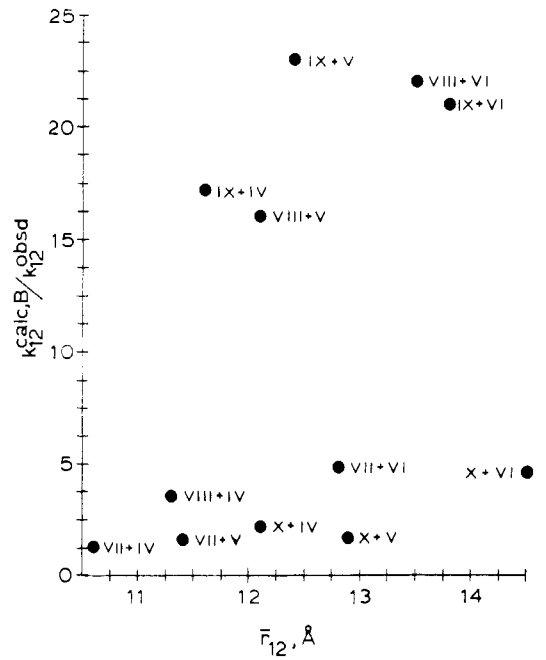

Figure 5. Plot of $k_{12}^{calcd}/k_{12}^{obsd}$ vs. $\bar{r}_{12}$ for the Cu(III) + Co(II) reactions. $\bar{r}_{12} = \bar{r}_{11} + \bar{r}_{22}$ (Table IV). Roman numerals indicate the reactants from Figure 1. Circles are for k_{12}^{calcd} according to assumption B (see Table V and text).

reactions, only the ratios using assumption B are displayed. Assumption B allows the self-exchange rate constants for the sterically hindered complexes to increase due to a diminution of $\Delta G^{**}_{11,out}$. For this reason, ratios of $k_{12}^{calcd}/k_{12}^{obsd}$ for reactions involving sterically hindered complexes are larger by using assumption B as opposed to assumption A. Nevertheless, Figure 4 clearly shows that the trends in the ratios with respect to $\bar{r}_{12}$ are nearly the same whether assumption A or B is used to calculate k_{12}. Trends in the ratios for the Cu(III) + Co(II) reactions are also similar whether assumption A or B is used. The ratios involving $k_{12}^{calcd,A}$ were omitted from Figure 5 for the sake of clarity.

Figure 4 clearly indicates that as the size of the organic substituents on the pyridine and phenanthroline ligands increases, the rates of electron transfer between the Ru(III) and Co(II) atoms decrease with respect to the calculated values. In addition to this general trend, it is interesting to examine Figure 4 for trends involving a single Ru(III) reactant with different Co(II) reactants and vice versa. For each Ru(III) complex, the ratio $k_{12}^{calcd}/k_{12}^{obsd}$ increases as the size of the Co(II) complex increases. The analogous trends involving one Co(II) complex and changing the size of the Ru(III) complex are less consistent except for $Co^{II}((bhm)_2phen)_3^{2+}$. These trends can be explained by hypothesizing that reactions involving the more sterically hindered complexes are increasingly nonadiabatic. Similar effects for self-exchange reactions involving substituted iron phenanthroline complexes have been reported.[6,36]

It is not obvious why nonadiabaticity, which is presumably caused by insufficient orbital overlap within the precursor complex, should manifest itself in reactions involving the ruthenium complexes. Since the organic substituents only affect the accessibility of the pyridine ligand, steric effects would only be important if interactions between pyridine and the Co(II) complex were necessary in the transition state. In a study of the reactions between various substituted pentaammine(pyridine)cobalt(III) complexes and ferrocyanide, Haim and coworkers concluded that electron transfer occurred through the ammine side of the Co(III) complex.[37] In addition, Beattie et al. found no evidence for steric effects when $Ru(NH_3)_5Cl^+$ was used to reduce tris(ethylenediamine)cobalt(III) and tris(cyclohexanediamine)cobalt(III).[42] Our results bear more resemblance to the studies of Cummins and Gray on the reaction of horse heart cytochrome *c* with $Ru(NH_3)_5(py)^{3+}$.[32] These authors concluded that interaction between the pyridine ligand and the partially exposed heme edge was required for adiabatic electron transfer. If a similar orientation is required in the reaction between the Ru(III) + Co(II) complexes discussed herein, it would explain the trends for the Ru(III) complexes and why those trends are more dramatic for the most hindered Co(II) complex, VI.

As shown in Figure 5, the trends in reactivity for the Cu(III) and Co(II) reactions are more complicated. With use of either assumption A or B, many of the reactions proceed at rates that are close to the calculated values. The reactions involving complex IX, $Cu^{III}(H_{-2}Aib_3)$, are all 15–25 times slower than predicted, and the reactions involving complex VIII, $Cu^{III}(H_{-2}A_3)$, with the more sterically hindered Co(II) complexes are also anomalously slow. Without the data for complex X, $Cu^{III}(H_{-2}Ach_3)$, it is tempting to attribute these trends to interactions involving α-methyl groups, but if this were true, the cyclohexyl groups in compound X would be expected to produce even larger effects. On the basis of our results, it is difficult to judge the importance of steric effects due to substituents in these reactions. The self-exchange reaction for complex X may be much faster than we predict, or the structure of the transition state for reactions involving complex X may be different from the structures for the other reactions. It should be noted that Margerum and co-workers found no evidence for steric effects in reactions between Cu(III) peptide complexes and Ru(II) complexes;[18] however, the probability of steric interactions in those reactions is not as great as for

(36) Chan, M. S.; Wahl, A. C. *J. Phys. Chem.* **1978**, *82*, 2542.
(37) Miralles, A. J.; Szecsy, A. P.; Haim, A. *Inorg. Chem.* **1982**, *21*, 697.
(38) Lim, H. S.; Barclay, D. J.; Anson, F. C. *Inorg. Chem.* **1972**, *11*, 1460.
(39) Haim, A.; Sutin, N. *Inorg. Chem.* **1976**, *15*, 476.
(40) Youngblood, M. P.; Margerum, D. W. *Inorg. Chem.* **1980**, *19*, 3068.
(41) The average radius, $\bar{r}$, represents the radius of a sphere that would have the same volume as the complex. The equations for the volume of a sphere, ellipsoid, and triangular prism are $V = 4\pi r^3/3$, $V = \pi(d_x d_y d_z)/6$, and $V = bhw/2$. By equating the appropriate volume equations and solving for r, one arrives at the equations for $\bar{r}$ given in the text.
(42) Beattie, J. K.; Binstead, R. A.; Boroccardo, M. *Inorg. Chem.* **1978**, *17*, 1822.

the reactions reported herein.

Use of Cross-Reaction Rate Constants for Probing Steric (Nonadiabatic) Effects in Electron-Transfer Reactions. In its complete form, Marcus' theory considers the possibility of nonadiabatic effects through a prefactor, p, in the expression for the rate constant. This prefactor is essentially a transmission coefficient. Equation 1 assumes an adiabatic transfer in which p is unity, whereas the more complete expression is

$$k_{12} = p_{12}Z_{12} \exp(-\Delta G^*_{12}/RT) \quad (16)$$

Sutin has pointed out that the use of eq 14, the correlation equation, will fail to identify nonunity prefactors as long as

$$p_{12} = (p_{11}p_{22})^{1/2} \quad (17)$$

where p_{11} and p_{22} express the nonadiabaticity in the appropriate self-exchange processes and if K_{12} is not large.[8] This result is fortuitous in that it aids in the application of the correlation equation, but the apparent success of eq 14 and 15 may be incorrectly used to justify the notion that most outer-sphere electron transfers are adiabatic.

The calculations that were used to construct Figures 2-5 were not susceptible to the problem discussed above because we used calculated as opposed to measured self-exchange rate constants for the sterically hindered complexes. The observed k_{11} values for these couples could be significantly less than the calculated values ($p_{11} < 1$), and if experimental values were known, the agreement between calculated and observed cross-reaction rate constants might be much better than it is.

Conclusions

Three series of structurally related redox couples based on $Ru(NH_3)_5(py)^{3+,2+}$, $Co(phen)_3^{3+,2+}$, and $Cu(H_{-2}G_3)^{0,-}$ have been prepared. In each series, the donor atoms and coordination geometry remain the same, but organic substituents of increasing size are introduced on the periphery of the ligands. The electronic spectra and electrochemical properties of the complexes indicate that organic substituents do not produce dramatic or unpredictable changes in these physical properties.

Rate constants for outer-sphere electron-transfer reactions between the Ru(III) and Co(II) and the Cu(III) and Co(II) complexes have been measured. The rate constants for both sets of reactions have the same dependence on driving force, and this dependence is close to the prediction of Marcus' theory. When the observed rate constants are compared to calculated values, the rates of reactions involving the complexes with the larger organic substituents appear to be attenuated, possibly due to nonadiabaticity. These trends are especially evident for the Ru(III) + Co(II) reactions, while the trends for the Cu(III) + Co(II) reactions are less straightforward.

In order to understand these steric effects it will be necessary to (i) synthesize additional ligands with even larger organic substituents, (ii) measure self-exchange rate constants for some of the complexes with large organic substituents, and (iii) determine activation entropies for some of the cross-reactions. These experiments are in progress in our laboratories.

Acknowledgment. This material is based upon work supported by the National Science Foundation under Grant 8204000. Acknowledgment is made to the donors of the Petroleum Research Fund, administered by the American Chemical Society, and to the Research Corp. for partial support of this research. The authors thank Arlene W. Hamburg for advice on synthesis and a sample of the peptide Aib_3 and Dale W. Margerum for useful discussions and a copy of his stopped-flow acquisition and analysis program.

Registry No. I^{2+}, 21360-09-8; II^{2+}, 19482-30-5; III^{2+}, 88326-60-7; IV^{2+}, 16788-34-4; V^{2+}, 47872-45-7; VI^{2+}, 88326-61-8; VII, 62801-36-9; VIII, 69042-71-3; IX, 69990-31-4; X, 88326-62-9.

Contribution from the Department of Chemistry, Purdue University, West Lafayette, Indiana 47907

Gas-Phase Reactions of Co^+ and Rh^+ with Toluene, Cycloheptatriene, and Norbornadiene

D. B. JACOBSON, G. D. BYRD, and B. S. FREISER*

Received December 10, 1982

The gas-phase reactions of toluene, cycloheptatriene, and norbornadiene with Co^+ and Rh^+ are described. The dominant process for Rh^+ is dehydrogenation, generating a $RhC_7H_6^+$ complex. These $RhC_7H_6^+$ ions decompose, yielding RhC^+ (benzene loss), presumably through the intermediacy of a carbide–benzene complex. Rh^+ dehydrogenates toluene-α,α,α-d_3 to eliminate both D_2 (70%) and HD (30%). Cobalt ions react quite differently with no $CoC_7H_6^+$ or CoC^+ observed. Both Co^+ and Rh^+ abstract hydride from cycloheptatriene, implying $D°(Co-H) > 38$ kcal/mol and $D°(Rh-H) > 47$ kcal/mol. The gas-phase chemistry of Rh^+ is similar to the chemistry observed on metal surfaces for cycloheptatriene and norbornadiene.

Introduction

The chemistry of various hydrocarbons on metal surfaces has been intensely studied with regard to catalytic processes.[1] In particular, the surface chemistry of several cyclic olefins and polyenes has been the focus of recent investigations.[2-7] An intriguing observation in these studies is the surface-mediated conversions of cycloheptatriene and norbornadiene to benzene.[6] The processes occurring on these metal surfaces are ill-defined. Concurrently, the study of gas-phase reactions of transition-metal ions with organic species has been rapidly expanding and is aimed at understanding the metal–organic interaction on a fundamental level.[8-10] Most of these studies have cen-

(1) Thomson, S. J. *Spec. Period. Rep.: Catalysis* **1977**, *1*.
(2) Tsai, M.-C.; Friend, C. M.; Muetterties, E. L. *J. Am. Chem. Soc.* **1982**, *104*, 2539.
(3) Tsai, M.-C.; Muetterties, E. L. *J. Phys. Chem.* **1982**, *86*, 5067.
(4) Tsai, M.-C.; Muetterties, E. L. *J. Am. Chem. Soc.* **1982**, *104*, 2534.
(5) Friend, C. M.; Muetterties, E. L. *J. Am. Chem. Soc.* **1981**, *103*, 773.
(6) Tsai, M.-C.; Stein, J.; Freind, C. M.; Muetterties, E. L. *J. Am. Chem. Soc.* **1982**, *104*, 3533.
(7) (a) Muetterties, E. L. In "Reactivity of Metal-Metal Bonds"; Chisholm, M. H., Ed.; American Chemical Society: Washington, DC, *ACS Symp. Ser. No. 155*, p 273. (b) Muetterties, E. L. *Chem. Soc. Rev.* **1982**, *11*, 283.
(8) (a) Allison, J.; Ridge, D. P. *J. Organomet. Chem.* **1975**, *99*, C11–C14. (b) Allison, J.; Ridge, D. P. *J. Am. Chem. Soc.* **1979**, *101*, 4998. (c) Allison, J.; Freas, R. B.; Ridge, D. P. *Ibid.* **1979**, *101*, 1332.
(9) (a) Armentrout, P. B.; Beauchamp, J. L. *J. Am. Chem. Soc.* **1981**, *103*, 784. (b) Armentrout, P. B.; Halle, L. F.; Beauchamp, J. L. *Ibid.* **1981**, *103*, 6624. (c) Armentrout, P. B.; Beauchamp, J. L. *Ibid.* **1981**, *103*, 6628. (d) Halle, L. F.; Armentrout, P. B.; Beauchamp, J. L. *Organometallics* **1982**, *1*, 984.
(10) (a) Burnier, R. C.; Byrd, G. D.; Freiser, B. S. *J. Am. Chem. Soc.* **1981**, *103*, 4360. (b) Byrd, G. D.; Burnier, R. C.; Freiser, B. S. *Ibid.* **1982**, *104*, 3565. (c) Jacobson, D. B.; Freiser, B. S. *Ibid.* **1983**, *105*, 736. (d) Jacobson, D. B.; Freiser, B. S. *Ibid.* **1983**, *105*, 5197.

0020-1669/84/1323-0553$01.50/0